

## EFFECT OF INTERACTION BETWEEN CLAY PARTICLES AND $\text{Fe}^{3+}$ IONS ON COLLOIDAL PROPERTIES OF KAOLINITE SUSPENSIONS

KUNSONG MA AND ALAIN C. PIERRE

University of Alberta, Edmonton, Canada

**Abstract**—Fine kaolinite suspensions were mixed with unaged or aged  $\text{FeCl}_3$  in this experiment. The interaction between clay particles and  $\text{Fe}^{3+}$  hydrolysis products was studied by transmission electron microscopy (TEM) and scanning electron microscopy (SEM). The proportion of Fe adsorbed was measured and the electrical charge on the clay particles was determined by electrophoresis. The effect of this interaction on flocculation of clay suspensions was investigated in a series of sedimentation tests. The  $\text{Fe}^{3+}$  ions acted as counterions when their concentration was low and when unaged  $\text{FeCl}_3$  solution was used. Otherwise, their hydrolysis complexes acted as a bonding agent between kaolinite particles. The dispersion–flocculation behavior of kaolinite suspensions was found to be in agreement with the theory of Derjaguin, Landau, Verwey and Overbeek (DLVO), as the sedimentation behavior could be predicted from the data of zeta potentials ( $\zeta$ ).

**Key Words**—Colloid, Electron Microscopy, Flocculation, Iron, Kaolinite, Sedimentation, Zeta Potential.

### INTRODUCTION

Understanding the interaction of metal ions with clays in aqueous media is of fundamental importance to controlling the ceramic process as well as the mining process. Since  $\text{Fe}^{3+}$  ions may be present naturally in clay minerals or can be added artificially into a pure clay, the interaction between  $\text{Fe}^{3+}$  ions and clays in aqueous media and the effect of the interaction on colloidal properties of a clay suspension have been studied extensively (Greenland 1975; Rengasamy and Oades 1977; Young and Ohtsubo 1987; Ma and Pierre 1992; Zou and Pierre 1992).

A clay—such as kaolinite, montmorillonite or illite—is an aluminosilicate mineral with platelike particles (Brindley 1958). The platelike particles have different crystal structures on their edges and faces. Thus, the electrical charges on edges are often different from that on faces. Clay particles interact in edge-to-edge (EE), edge-to-face (EF) and face-to-face (FF) modes and form a “card-house” structure in aqueous media (van Olphen 1977). However, the structure characterization or the colloidal behavior depends largely on the nature of the clay and other aqueous medium.

The behavior of  $\text{Fe}^{3+}$  ions is very complicated in aqueous media, and has been reviewed by Henry et al. (1990) and Livage et al. (1988).  $\text{Fe}^{3+}$  ions undertake a series of chemical reactions through complexation, hydrolysis and condensation in aqueous media to form different Fe hydroxylated species, precipitates and gels over specific pH ranges. These chemical products interact with clay particle surfaces and change the electrical properties of clay particles in aqueous media significantly. Therefore, the dispersion–flocculation behavior of clay suspensions is exceedingly complex in the presence of  $\text{Fe}^{3+}$  ions

(Blackmore 1973; El-Swaify and Emerson 1975; Rengasamy and Oades 1977; Young and Ohtsubo 1987)

In a previous study (Ma and Pierre 1992), the sedimentation behavior of a fine kaolinite suspension in the presence of  $\text{Fe}^{3+}$  electrolytes was systematically investigated in aqueous media. The sedimentation behavior was explained qualitatively in terms of DLVO theory (Verwey and Overbeek 1948; Hiemenz 1977). It was shown that when the repulsion of 2 electrical double layers around kaolinite particles was strong, the colloidal system remained dispersed. As the  $\text{Fe}^{3+}$  concentration increased, the electrical double layer was compressed. Consequently, the dispersed kaolinite suspension was flocculated.

In the present study, the interaction between clay particles and  $\text{Fe}^{3+}$  ions was examined in more detail. The variation of the electrical charge of kaolinite particles as a function of pH and  $\text{Fe}^{3+}$  concentration was measured. The supercritical drying technique was applied to make clay sediment samples with original structure. The linkage between clay particles was observed by electron microscopy. The results are reported in the following paragraphs.

### EXPERIMENTAL

Hydrite UF kaolinite from Georgia Kaolin Company was used in this study. The median particle size was 0.20  $\mu\text{m}$  (Georgia Kaolin Company 1990). This kaolinite was processed by acidified salt washes (Rand and Melton 1977), following the Schofield and Samson (1954) method, to remove adsorbed impurities and convert the kaolinite to sodium form. Before any sedimentation experiment, a 0.125 M  $\text{Na}_4\text{P}_2\text{O}_7$  solution was added to the kaolinite suspension so as to disperse it, in a ratio of 1 mL solution to 0.5 g kaolinite. This

kaolinite was charged negatively on both edges and faces (Ma 1995).

Two types of  $\text{FeCl}_3$  solutions were used in this study. In the first type,  $\text{FeCl}_3$  was dissolved in distilled water at room temperature, and added to the kaolinite suspensions just before a sedimentation experiment. This type of aqueous  $\text{FeCl}_3$  solution is called “unaged” throughout this paper. The other type of solution is called “aged”, and it was prepared by the following procedure. The  $\text{FeCl}_3$  was dissolved in distilled water at room temperature at a concentration of 1.0 M. This solution was allowed to age for 1 mo before it was mixed with a kaolinite suspension. Precipitation occurred during aging. A part of the precipitate was collected and dried in a desiccator for X-ray diffraction (XRD) analysis.

Kaolinite suspensions were prepared in graduated glass cylinders with an inside diameter of 28 mm. The Na-kaolinite content was 0.5 g in each cylinder. The sedimentation experiments were carried out at pH 2, 4, 6, 8, 9.5, 10 and 11 with unaged  $\text{FeCl}_3$  and at pH 2, 4, 6, 9.5 and 11 with aged  $\text{FeCl}_3$ . The pH values of the suspensions were adjusted with diluted HCl or NaOH. Then  $\text{FeCl}_3$  solution was added to the cylinders. At each pH level, 6 concentrations of unaged  $\text{FeCl}_3$  were examined: 0.0, 0.17, 0.33, 0.67, 1.67 and 3.33 mM, respectively, and 6 concentrations of aged  $\text{FeCl}_3$ : 0.33, 0.67, 1.67, 3.33, 5.00 and 10.00 mM, respectively. The initial volume of the suspension in a cylinder was 100 mL after it was adjusted to a required pH value and the concentration of  $\text{FeCl}_3$ . Each cylinder was covered with a piece of parafilm, then shaken vigorously to homogenize the clay suspension. All sedimentation tests were carried out at room temperature. When a clear interface was formed in a suspension, the position of this interface was recorded. The final sediment thickness was defined as the thickness after 360-h sedimentation. A height of 1 cm corresponded to a volume of 6.16 mL in a graduated cylinder.

In order to observe the structure of the kaolinite sediments under SEM, the samples were dried by the supercritical method. This technique is efficient to eliminate capillary force on samples during drying and to preserve the original structure of the sediments that were formed. To do this, some suspension samples were transferred from a glass cylinder to dialysis tubes from the Spectrum Company and sedimentation was carried out in these tubes. After sedimentation was complete, the dialysis tubes were allowed to make a very slow liquid exchange for ethanol. Then the dialysis tubes were placed in a supercritical point dryer (Bio-Rad E3000 Series). In this dryer, ethanol was replaced by liquid  $\text{CO}_2$ . The temperature and pressure of  $\text{CO}_2$  were raised above critical point values ( $T_c = 31^\circ\text{C}$  and  $P_c = 74.433\text{ kPa}$  (Smart and Tovey 1982)),

where it was evacuated. Finally, the supercritical-dried samples were examined under a Hitachi S-2700 SEM.

For TEM observation, a diluted clay suspension was dropped on a carbon-coated copper grid supplied by the SPI Company. A JEOL-2010 analytical transmission electron microscope (ATEM) with an X-ray detector was used in this study.

The electrophoretic measurements were performed with a particle micro-electrophoresis MARK II apparatus from the Rank Brother Company. This piece of equipment had a flat and rectangular cell. The electrophoretic mobility of a minimum of 5 particles was successively measured, first when applying the electric field in 1 direction, then after reversing the direction of the applied electric field. For the equipment being used, the zeta potential could be calculated from the following formula (Plitt 1993):

$$\zeta = \frac{4\pi\eta u}{\epsilon E} \times (300)^2 \quad [11]$$

where  $\zeta$  is the zeta potential in V,  $\eta$  is the liquid viscosity in poise,  $\epsilon$  is the relative dielectric constant of the liquid (as an approximation, the viscosity and dielectric constant of water were used),  $u$  is the average velocity of clay particles in cm/s and  $E$  is the electric field in V/cm. For the cell being used,  $E = V/3.27$  where  $V$  is the applied voltage.

Because the original concentration (0.5% by mass) of kaolinite suspensions was too dense to directly measure their zeta potential, the suspensions were diluted to a concentration of 0.05% (by mass) with distilled water. In each case, just before measuring the zeta potential, the pH was adjusted to the value that the suspension had before dilution, with a HCl or NaOH solution. Depending on the sample, unaged or aged  $\text{FeCl}_3$  solution was added to the clay suspension so as to maintain the initial electrolyte concentration existing before dilution.

The Fe concentration present in the supernatant liquid of clay suspensions was measured by atomic absorption (AA) with a Perkin-Elmer 4000AAS AA spectrophotometer. The samples analyzed were prepared in the same way as those for sedimentation, and we waited 12 h before performing an analysis. In clay suspensions where flocculation occurred, the Fe content in the clear supernatant liquid was analyzed directly. In clay suspensions where flocculation did not occur, the suspension was centrifuged until a clear supernatant liquid separated from the suspension.

## RESULTS

The sedimentation behavior of kaolinite suspensions could be classified into 3 types: 1) accumulation sedimentation; 2) flocculation sedimentation; and 3) mixed accumulation–flocculation sedimentation. As an example, the dynamics of kaolinite sedimentation in the presence of unaged and aged  $\text{FeCl}_3$  at pH 4 are

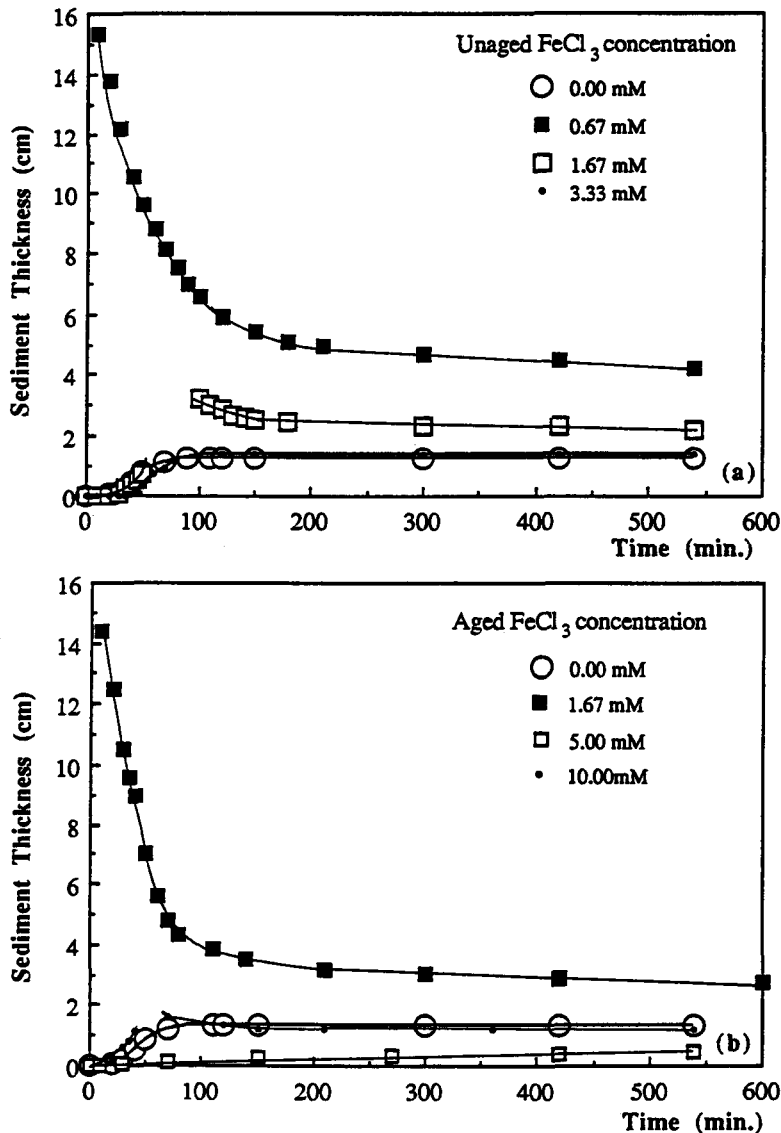


Figure 1. Sediment kinetics of 0.5% Na-kaolinite suspensions at pH 4; a) displacement of sharp interfaces with unaged  $[\text{FeCl}_3] = 0, 0.67, 1.67$  and  $3.33 \text{ mM}$ ; b) displacement of sharp interfaces with aged  $[\text{FeCl}_3] = 0, 1.67, 5.00$  and  $10.00 \text{ mM}$ .

reported in Figures 1a and 1b, respectively. Typical accumulation sedimentation occurred when a relatively stable suspension was achieved, such as that without any  $\text{FeCl}_3$  and with unaged  $\text{FeCl}_3$  concentration of  $3.33 \text{ mM}$  or with aged  $\text{FeCl}_3$  concentration of  $5.00 \text{ mM}$ . Heaviest particles settled first under gravity and the sediment was established at the bottom of a cylinder. The thickness of the sediment increased as sedimentation time lapsed. Typical flocculation sedimentation occurred with unaged  $\text{FeCl}_3$  concentration of  $0.67 \text{ mM}$  or with aged  $\text{FeCl}_3$  concentration of  $1.67 \text{ mM}$ . A sharp interface between the sediment and the clear supernatant liquid was observed and this interface kept moving downward until equilibrium was established.

Mixed flocculation–accumulation sedimentation was observed in the suspensions with unaged  $\text{FeCl}_3$  concentration of  $1.67 \text{ mM}$  or with aged  $\text{FeCl}_3$  concentration of  $10.00 \text{ mM}$ . In this case, sedimentation followed the dynamic of an accumulation sedimentation at the beginning. Then it acted like that of a flocculation sedimentation. These different kinds of sedimentation behaviors were characterized in Ma and Pierre (1992).

Figure 2 shows the final sediment thickness of suspensions with different concentrations of unaged and aged  $\text{FeCl}_3$  at pH 2 and 9.5. At pH 2, both with unaged or aged  $\text{FeCl}_3$ , flocculation sedimentation occurred, while accumulation sedimentation occurred at pH 9.5. In both cases, the final sediment thickness increased

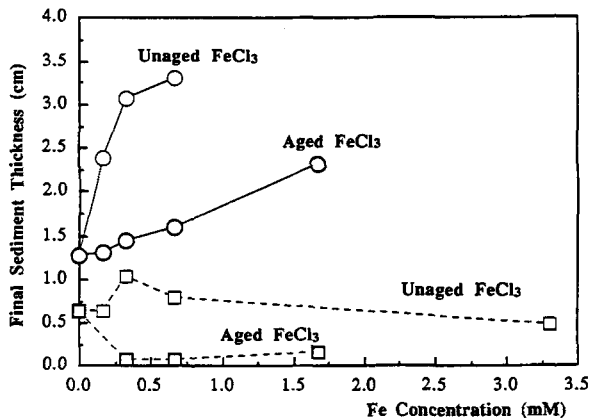


Figure 2. Sedimentation behavior of 0.5% Na-kaolinite suspensions as a function of the concentration of unaged or aged  $\text{FeCl}_3$ . The solid lines represent the final sediment thickness by flocculation sedimentation at pH 2; the dashed lines represent the final sediment thickness by accumulation sedimentation at pH 9.5.

with the concentration of unaged or aged  $\text{FeCl}_3$ . Unaged  $\text{FeCl}_3$  increased the thickness more effectively than aged  $\text{FeCl}_3$ .

When unaged  $\text{Fe}^{3+}$  electrolytes were mixed with kaolinite suspensions, the  $\text{Fe}^{3+}$  ions undertook hydrolysis in the aqueous media. Ferric hydrolysis compounds did precipitate on the clay particle surfaces, and Figures 3a and 3b show the TEM observations of interaction of such hydrolysis products with kaolinite particles. The energy dispersive X-ray (EDX) analyses of selected areas, represented by small circles in Figures 3a and 3b, are also reported in Figures 3c and 3d. The Fe precipitates had the appearance of rodlike or platelike particles (Figure 3a), eventually joining to each other to form a thin film (Figure 3b). The corresponding EDX analysis indicated that these particles and films were Fe compounds.

We mentioned previously that precipitation occurred in  $\text{FeCl}_3$  solutions during aging. The XRD analysis indicated that these precipitates included ferric hydroxides ( $\text{FeOOH}$ ) and ferric oxides (hematite  $\text{Fe}_2\text{O}_3$  and  $\text{Fe}_2\text{O}_3 \cdot \text{H}_2\text{O}$ ) (Ma 1995). By AA analysis, we found

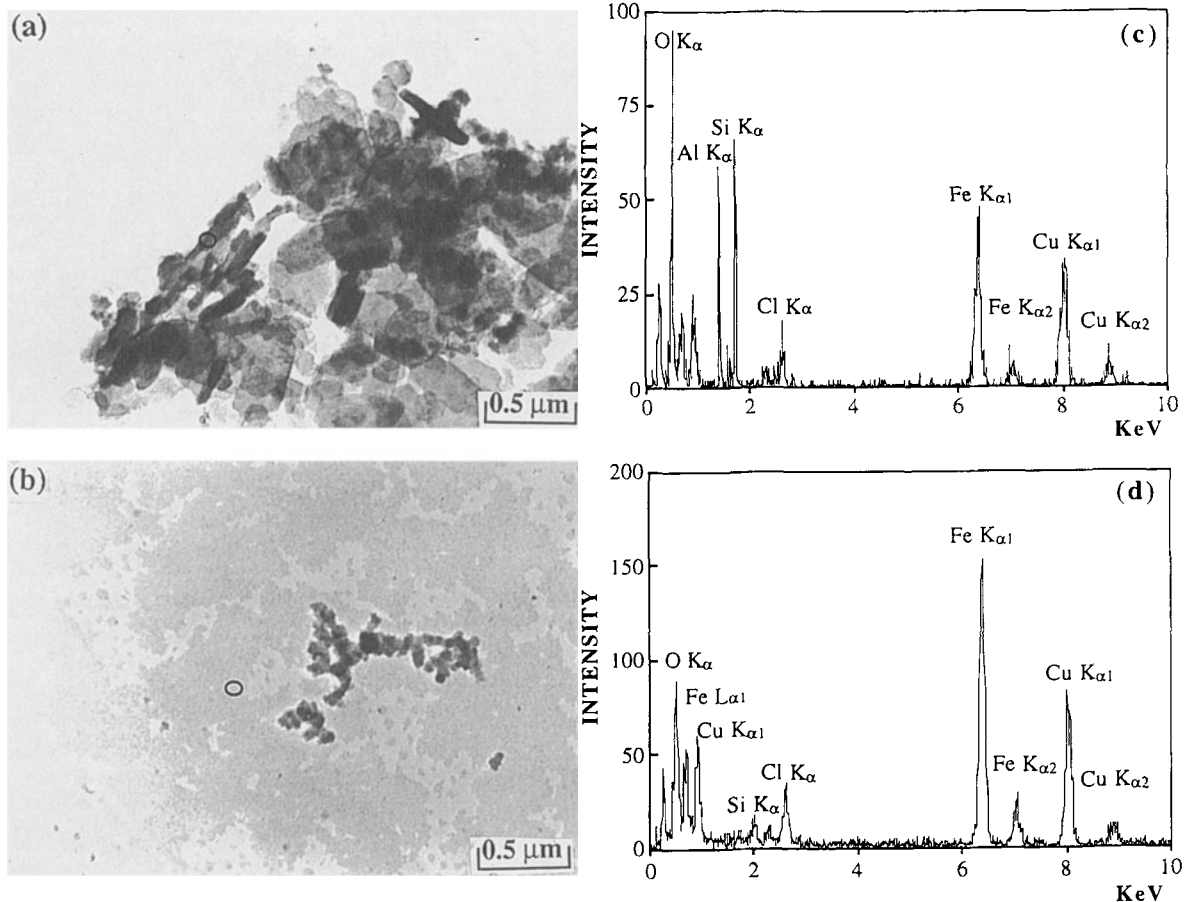


Figure 3. TEM micrographs of the Fe materials deposited on the kaolinite particles in sediments made with 10 mM  $\text{FeCl}_3$  at pH 9.5: a) rodlike and platelike particles; b) thin film; c) EDX spectrum of the surface of the kaolinite particles corresponds to circle in (a); and d) EDX spectrum on the surface of the kaolinite particles corresponds to circle in (b).

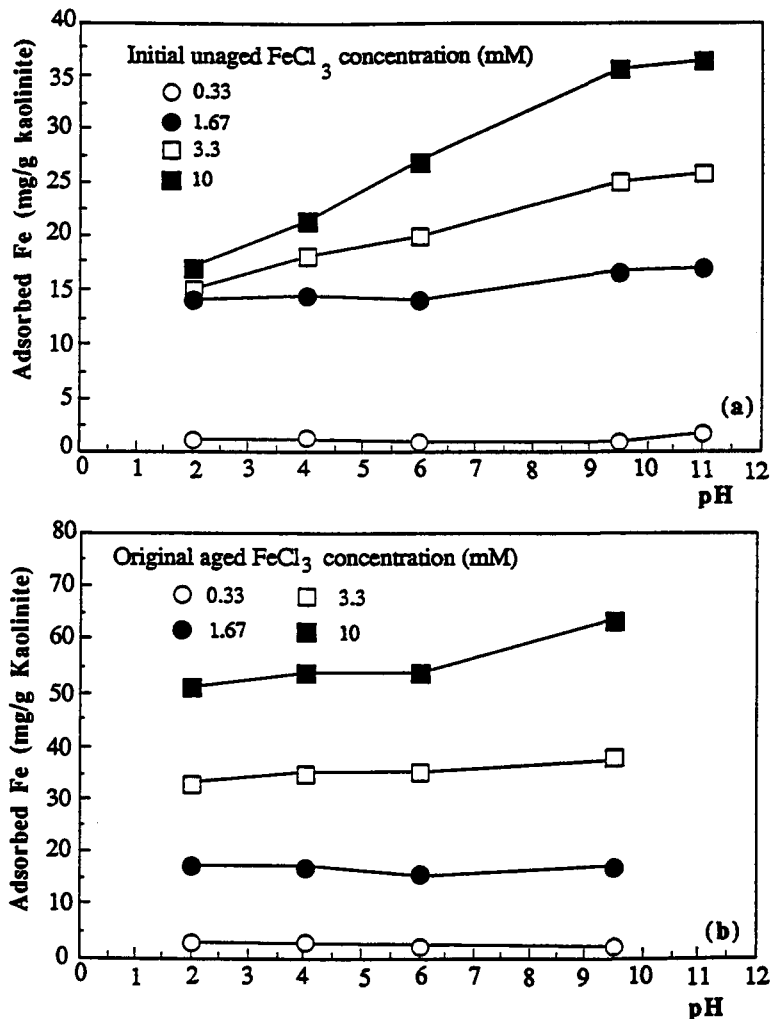


Figure 4. Amount of Fe deposited on the kaolinite particles from  $\text{FeCl}_3$ , at different pH: a) from unaged  $\text{FeCl}_3$ ; b) from aged  $\text{FeCl}_3$ .

that Fe concentration in the liquid had decreased from 0.5 to 0.33 M. In clay suspensions mixed with aged  $\text{FeCl}_3$  solution, ferric hydroxides and ferric oxides deposited on the clay particles. The amount of Fe deposited on the kaolinite particles, as a function of pH and concentration of unaged  $\text{FeCl}_3$  or aged  $\text{FeCl}_3$ , is reported in Figure 4. It appears that the amount of Fe deposited on kaolinite particles from unaged  $\text{FeCl}_3$  increased with the initial Fe concentration and pH. On the contrary, the amount of deposited Fe from aged  $\text{FeCl}_3$  was almost independent of the pH.

When the pH and  $\text{Fe}^{3+}$  concentrations in clay suspensions were changed, the association mode of clay particles changed. Figure 5 shows the SEM observations after a supercritical drying of kaolinite sediments made with different concentrations of unaged  $\text{FeCl}_3$  at different pH. Without any  $\text{FeCl}_3$  at pH 9.5 (Figure 5a), clay particles were compacted. Most of the particles

were connected randomly. Without any  $\text{FeCl}_3$  at pH 4.0 (Figure 5b), the sediment was relatively dense. Some kaolinite particles appeared to be randomly connected. However, FF and EE associations can also be observed. With the unaged  $\text{FeCl}_3$  concentration of 0.67 mM at pH 4.0 (Figure 5c), the sediment was very loose. Most clay particles were associated in the EE mode. With a higher unaged  $\text{FeCl}_3$  concentration (3.33 mM) at pH 4.0, Figure 5d shows a very densely packed structure. Almost all of the kaolinite particles were associated in the FF mode.

Figures 6a and 6b show the dependence of zeta potentials on the pH and concentrations of unaged and aged  $\text{FeCl}_3$  in kaolinite suspensions. The zeta potentials increased with the concentration of unaged or aged  $\text{FeCl}_3$  at all pH values. However, the addition of unaged  $\text{FeCl}_3$  resulted in a faster increase of the zeta potential than aged  $\text{FeCl}_3$  did.

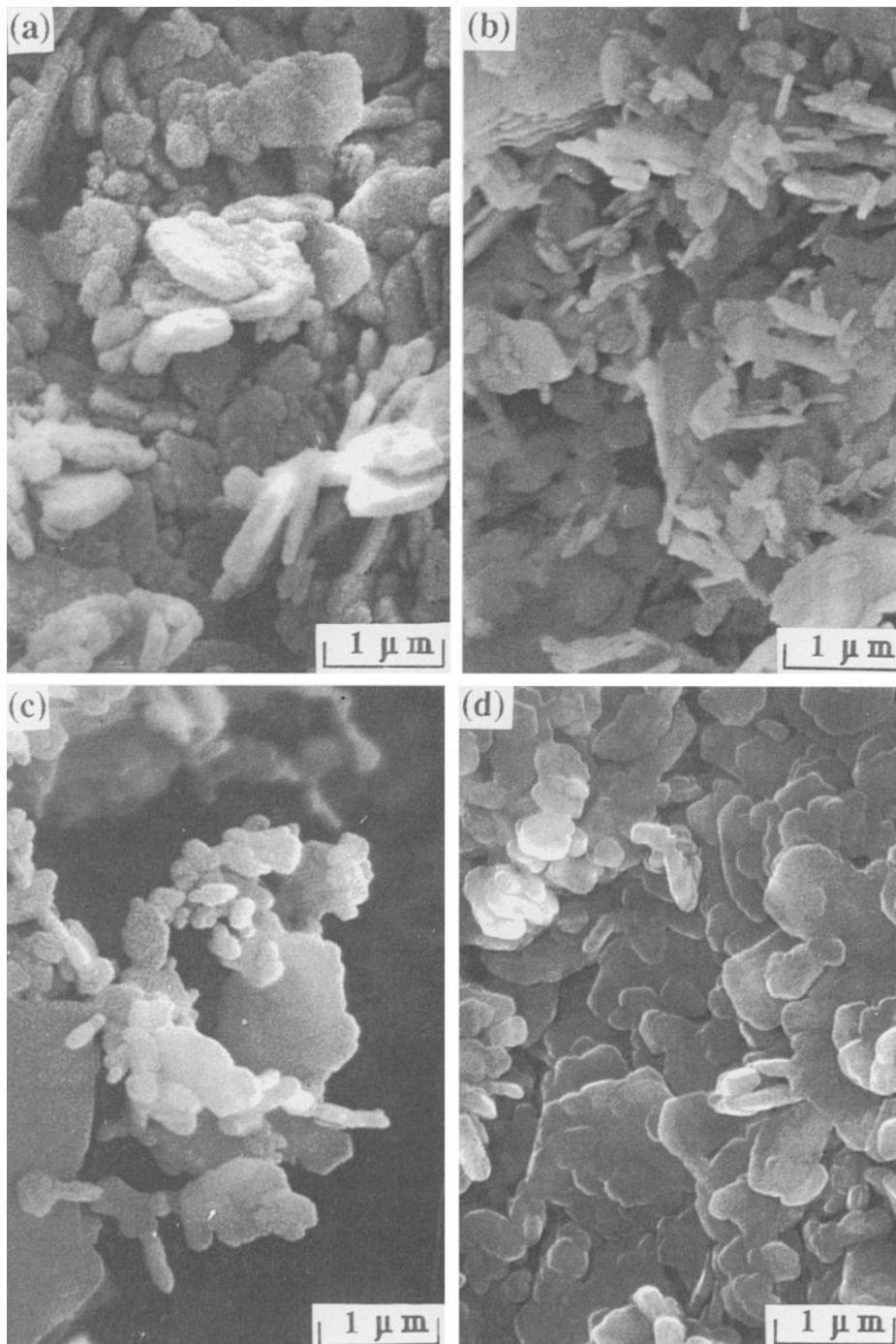


Figure 5. SEM micrographs of kaolinite sediments made at 10 kV: a) the accumulated kaolinite sediment without  $\text{FeCl}_3$  at pH 9.5; b) the accumulated kaolinite sediment without  $\text{FeCl}_3$  at pH 4; c) the flocculated kaolinite sediment made at pH 4 with unaged  $\text{FeCl}_3$  at a concentration of 0.67 mM; d) the accumulated kaolinite sediment made at pH 4 with unaged  $\text{FeCl}_3$  at a concentration of 3.33 mM.

The observed sedimentation behavior of kaolinite suspensions with unaged  $\text{FeCl}_3$  is summarized in Figure 7a, while that for aged  $\text{FeCl}_3$  is summarized in Figure 8a. Dashed lines were drawn to outline the

range of conditions where each type of sedimentation occurred. From the determined values of zeta potential, a diagram showing 3 domains could be established according to the following standards: 1) The

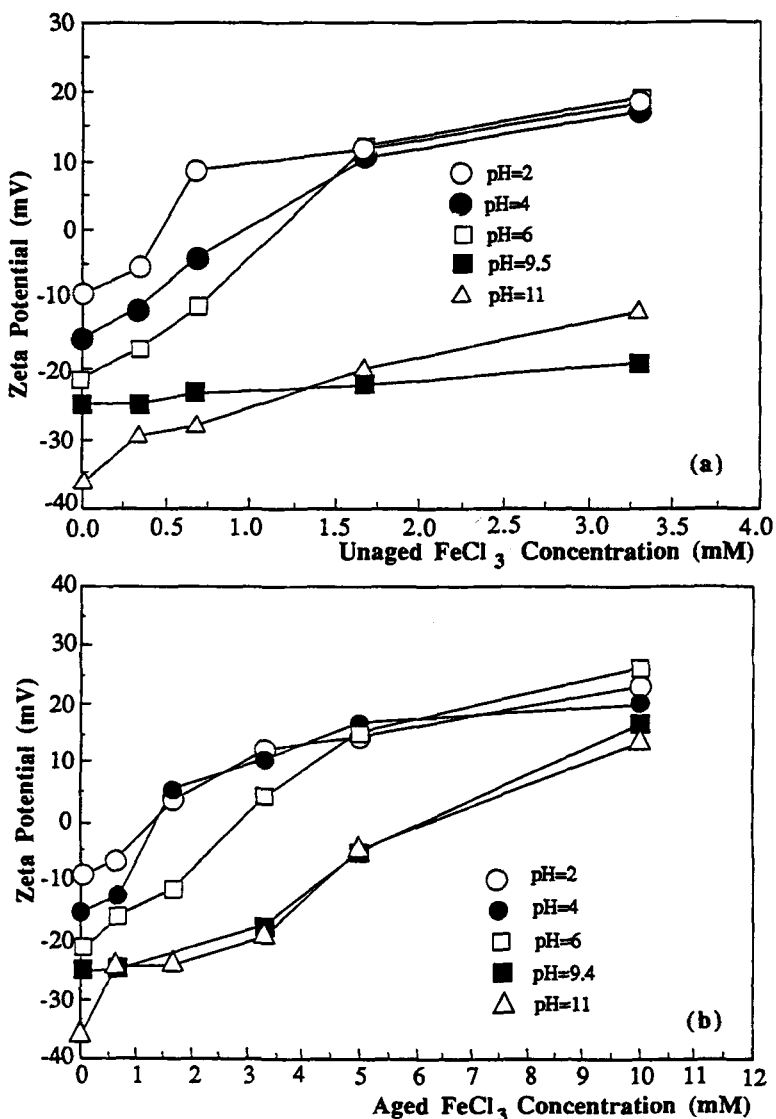


Figure 6. Variation of the zeta potential with the concentration of  $\text{FeCl}_3$  at different pH values in 0.5% kaolinite suspensions treated with  $\text{Na}_4\text{P}_2\text{O}_7$ : a) unaged  $\text{FeCl}_3$ ; b) aged  $\text{FeCl}_3$ .

first domain, with data points represented by open dots, corresponds to a zeta potential absolute value  $|\zeta| < 10$  mV. 2) The second domain, with data points represented by solid dots, corresponds to  $|\zeta| > 15$  mV. 3) The third domain, represented by semi-open dots, corresponds to data points such that  $10 \text{ mV} \leq |\zeta| \leq 15$  mV. These diagrams from the zeta potential are reported in Figure 7b for kaolinite suspensions with unaged  $\text{FeCl}_3$  and in Figure 8b with aged  $\text{FeCl}_3$ . When comparing Figure 7a with 7b or Figure 8a with 8b, it appears that the diagrams constructed from the zeta potential are similar to those from the experimental sedimentation behaviors.

## DISCUSSION

In the present study, the sedimentation behaviors of kaolinite suspensions were classified into several types. Since kaolinite particles have a platelike shape, these particles can be associated in the 3 basic fashions: EF, EE and FF, which were summarized by van Olphen (1977). The SEM observations of sediments clearly show that the different sedimentation behaviors were related to the different architectures of clay aggregates, depending on the concentration of  $\text{Fe}^{3+}$  and pH (Figure 5). The present important result is that the sedimentation behaviors of kaolinite suspensions appeared to be predictable from the value of the zeta

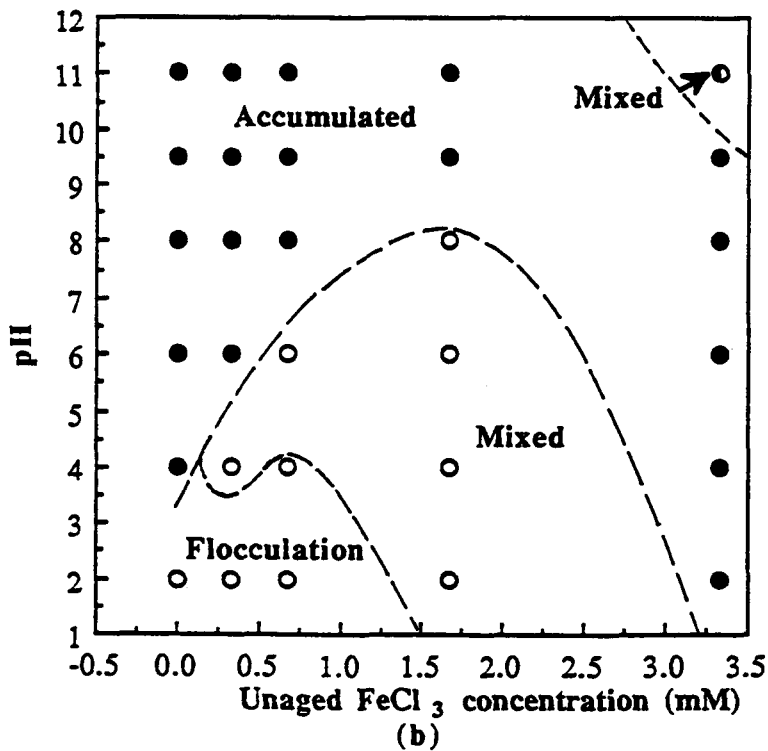
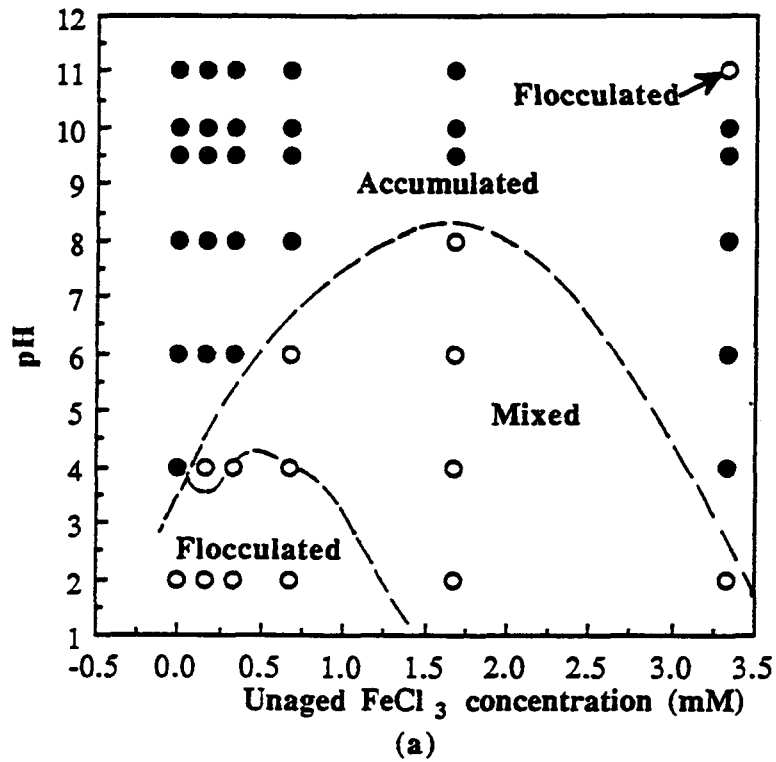


Figure 7. Diagram of the sedimentation behavior in 0.5% kaolinite suspensions mixed with unaged  $\text{FeCl}_3$ : a) observed results; b) predictions from the measured zeta potential,  $\zeta$ . The open dots are for  $|\zeta| < 10$  mV, the solid dots for  $|\zeta| > 15$  mV, the semi-open dots for  $10 \text{ mV} \leq |\zeta| \leq 15$  mV.



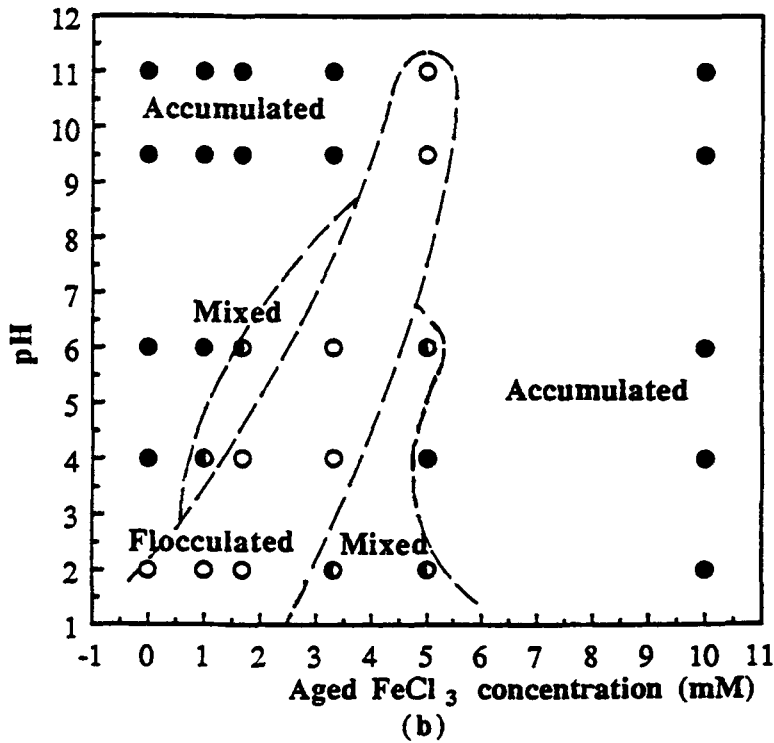
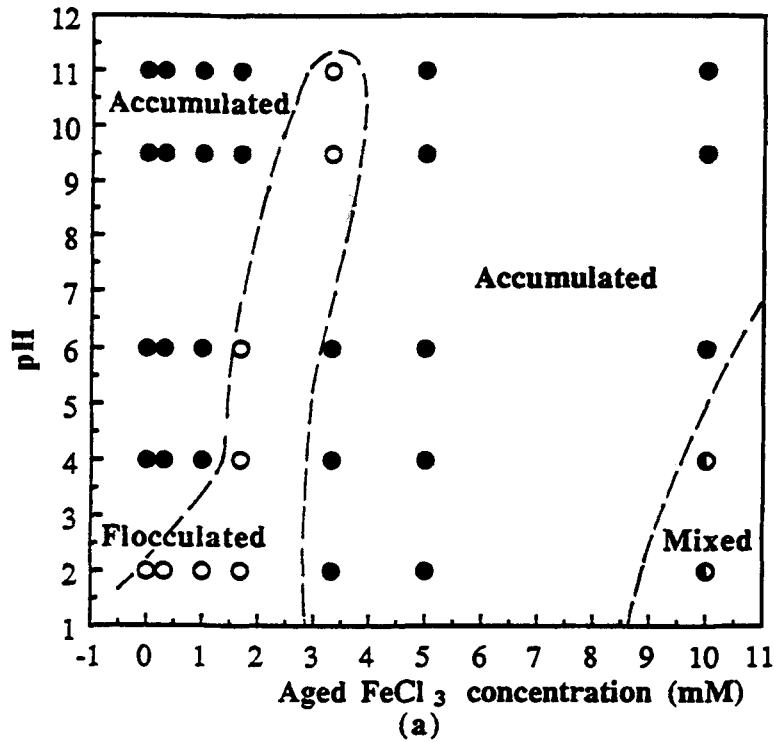


Figure 8. Diagram of the sedimentation behavior in 0.5% kaolinite suspensions mixed with aged FeCl<sub>3</sub>: a) observed results; b) predictions from the measured zeta potential,  $\zeta$ . The open dots are for  $|\zeta| < 10$  mV, the solid dots for  $|\zeta| > 15$  mV, the semi-open dots for  $10 \text{ mV} \leq |\zeta| \leq 15$  mV.

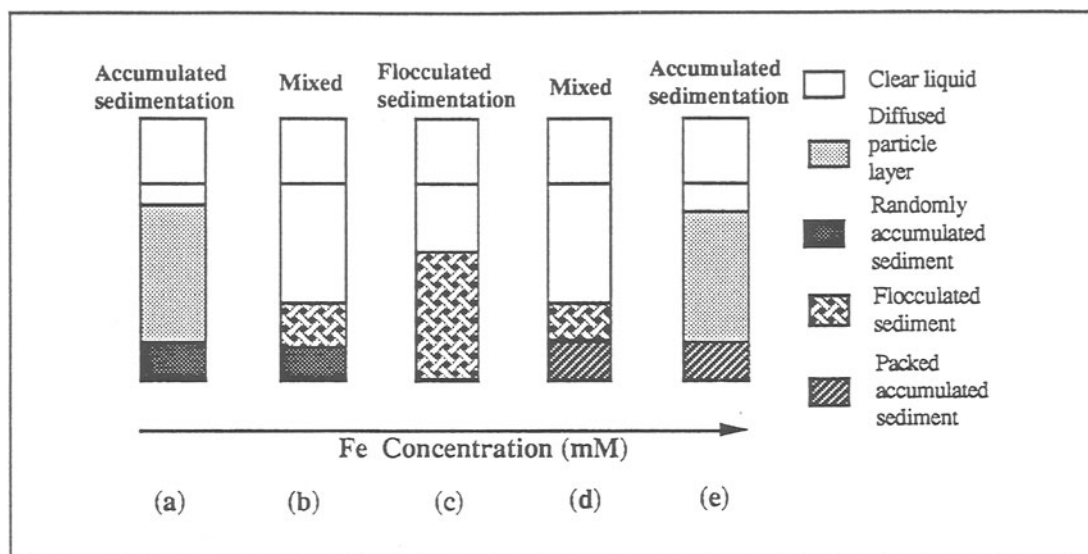


Figure 9. Schematic illustration of variations in the sedimentation behavior of diluted fine kaolinite suspensions with the Fe concentration.

potential. This is to say, the dispersion or flocculation behavior of clay particles was globally consistent with the DLVO theory.

In the present study, kaolinite was treated with  $\text{Na}_4\text{P}_2\text{O}_7$  so that the platelike particles were negatively charged both on their edges and faces. Hence,  $\text{Fe}^{3+}$  acted as counterions to the clay particles, and it is possible to argue that several types of sedimentation behavior, due to a changing mode of particle association, should occur as the concentration of  $\text{Fe}^{3+}$  increases. These types of sedimentation behaviors are illustrated in Figure 9.

Without  $\text{Fe}^{3+}$  or with a low  $\text{Fe}^{3+}$  concentration in clay suspensions at a high pH, clay particles had a relatively high surface potential (in absolute magnitude) and a thick electrical double layer (Figure 6a). That is to say, a strong repulsion between the clay particles operated. No aggregation occurred and the clay suspensions were stable. Only accumulation sedimentation occurred (Figure 9a). During sedimentation, the heaviest particles settled first under gravity and then the smaller particles took a long time to settle. The clay particles formed an accumulated sediment at the bottom of a cylinder. The sediment was relatively dense. In terms of the particle association mode, random packing occurred (Figure 5a).

As the  $\text{Fe}^{3+}$  concentration increased, the  $\text{Fe}^{3+}$  counterion compressed the electrical double layer around the clay particles. Thus, the magnitude of the zeta potential was significantly reduced. When  $-10 \text{ mV} < \zeta < 0 \text{ mV}$ , the EE association of the clay particles was favored according to theoretical calculations based on the DLVO theory (Ma 1995). The clay suspensions were unstable and only flocculation sedimentation oc-

curred (Figures 6a and 7a). During flocculation sedimentation, as suggested by Michaels and Bolger (1962), clay particles formed very porous flocs, and these flocs joined to each other, from wall to wall in the glass cylinder, so as to constitute an apparently uniform sediment, separated by a sharp interface from the clear supernatant liquid. The sediment kept shrinking during sedimentation, but it would still occupy a significantly large space after a long time, in agreement with the present experiment (Figures 2 and 5c).

However, the transition from flocculation sedimentation to accumulation sedimentation was progressive. In some  $\text{Fe}^{3+}$  concentrations and pH levels, accumulation sedimentation was in competition with flocculation sedimentation so that a mixed sedimentation was observed (Figure 9b). The heaviest kaolinite particles settled quickly at the beginning so that the sedimentation process appeared by accumulation. After a while, the remaining particles had time to flocculate. They formed a flocculated sediment, so that the second step of sedimentation was by flocculation. Finally, the sediment was composed of a randomly accumulated sediment at the bottom of the glass cylinder and a flocculated sediment over it.

$\text{Fe}^{3+}$  ions are strongly hydrolyzed in aqueous media. Depending on the pH, a  $\text{FeCl}_3$  solution may contain monomers such as  $[\text{Fe}(\text{OH})(\text{OH})_2]^{2+}$  or polycations such as  $[\text{Fe}_4\text{O}_3(\text{OH})_4]^{2n+}$ . The precipitates that can be formed include  $\alpha\text{-FeO}(\text{OH})$  and  $\beta\text{-FeO}(\text{OH})$ , and the oxide  $\alpha\text{-Fe}_2\text{O}_3$  (Livage et al. 1988; Henry et al. 1990), depending on the pH. As mentioned by Blackmore (1973), these hydrolysis products can themselves adsorb onto clay particles (Figure 4) and coat their surface (Figure 3). Since the point of zero charge (p.z.c.)

of Fe minerals is in a range from 7 to 9 (Schwertmann and Taylor 1989), the sign of electric charges of clay particles can reverse when the Fe<sup>3+</sup> concentration increases, in agreement with our result (Figure 6a). In this case, the Fe<sup>3+</sup> hydrolysis species are no longer counterions to the clay particles. Rather, they can act as a bonding agent to bridge kaolinite particles to each other. Our observations are consistent with this view as they showed that the kaolinite particles were associated mostly according to the FF mode. Consequently, dense aggregates formed and they easily settled under gravity. The formation of a very dense or packed accumulated sediment was observed. In the sedimentation test, a new transition from flocculation sedimentation to accumulation sedimentation (Figure 9e) was observed as the FeCl<sub>3</sub> concentration increased. Again, competition between flocculation sedimentation and accumulation sedimentation was observed for intermediate conditions (Figure 9d). In this case, the sediment was composed of a packed accumulated sediment at the bottom of the glass cylinder and a flocculated sediment over it.

The above evolution in the architecture of clay sediments as the Fe concentration increased was confirmed when aged FeCl<sub>3</sub> was used. If the sedimentation behaviors with unaged and aged FeCl<sub>3</sub> are compared, it appears that the field of conditions where accumulation sedimentation occurred was enlarged with aged FeCl<sub>3</sub> toward low Fe concentration and high pH (Figures 7a and 8a). In fact, the Fe amount adsorbed onto the clay particles was lower from unaged than from aged FeCl<sub>3</sub> (Figure 4). Also, the Fe amount adsorbed by kaolinite from unaged FeCl<sub>3</sub> depended on the pH, because an increasing pH is known to accelerate the hydrolysis of Fe<sup>3+</sup> ions. However, the hydrolyzed process of Fe<sup>3+</sup> was completed after aging so that the amount of Fe-adsorbed Fe on kaolinite was eventually independent of the pH. Partially, the population of highly charged Fe species in solution was less with aged Fe electrolyte solutions than with unaged solution. Consequently, the electrical double layer was less compressed with the aged Fe electrolytes. In turn, the very porous floc with the EE association was less frequent with the aged Fe electrolytes. As a result of this difference, the final sediment volume was always higher with unaged than with aged FeCl<sub>3</sub> (Figure 2). However, since the aged Fe electrolytes coated the kaolinite particles more easily (Figure 4), the electrical charge on the particles changed sign for a lower amount of aged than unaged FeCl<sub>3</sub>. Also, the zeta potential increased faster with the aged Fe electrolytes, which explains that packed accumulation sedimentation occurred with a lower concentration of aged than unaged FeCl<sub>3</sub> (Figures 7a and 8a).

In summary, the sedimentation behavior of the kaolinite suspensions could first be qualitatively explained in terms of the DLVO theory, as a function of

the Fe concentration. Secondly, the data of zeta potentials could be used to predict the type of sedimentation behaviors. In practice, flocculation sedimentation occurred when  $|\zeta| < 10$  mV, accumulation sedimentation when  $|\zeta| > 15$  mV, and mixed flocculation–accumulation sedimentation when  $10 \text{ mV} \leq |\zeta| \leq 15 \text{ mV}$ .

## CONCLUSION

The present study showed that Fe<sup>3+</sup> and the hydrolysis products acted as counterions to flocculate clay particles when the particles were charged negatively on both their edges and faces. These Fe products also acted as a bonding agent to connect the clay particles. The sedimentation in kaolinite suspensions can occur according to 1 of the following 3 behaviors: 1) accumulation; 2) flocculation; or 3) mixed flocculation–accumulation. The different types of clay particle associations observed under the electron microscope were consistent with their sedimentation behaviors. This sedimentation behavior could be explained according to the DLVO theory and related to the value of the zeta potentials of the clay particles.

The current results can be used to improve the castability and sinterability of ceramics products. Also, they are applicable in environmental science and engineering, such as in the treatment of oil sand tailing sludge.

## ACKNOWLEDGMENTS

The authors are very grateful to the Natural Sciences and Engineering Research Council of Canada (NSERC) for funding this research on an operating grant.

## REFERENCES

- Blackmore AV. 1973. Aggregation of clay by the products of iron(III) hydrolysis. *Aust J Soil Res* 11:75–82.
- Brindley GW. 1958. Clays and clay raw materials. In: Kingery WD, editor. *Ceramic fabrication processes*. New York: MIT and J. Wiley. p 7–22.
- El-Swaify SA, Emerson WW. 1975. Changes in the physical properties of soil clays due to precipitated aluminum and iron hydroxides. I: Swelling and aggregate stability after drying. *Soil Sci* 39:1056–1063.
- Georgia Kaolin Company, Inc. 1990. Information about properties of hydrite UF kaolinite particles, Georgia Kaolinite Company, Union, New Jersey.
- Greenland DJ. 1975. Charge characteristics of some kaolinite–iron hydroxide complexes. *Clay Miner* 10:407–416.
- Henry M, Jolivet JP, Livage J. 1990. Aqueous chemistry of metal cation: Hydrolysis, condensation, and complexation. *Structure and Bonding* 25:1–64.
- Hiemenz PC. 1977. *Principles of colloidal and surface chemistry*. New York: Marcel Dekker. 815 p.
- Livage J, Henry M, Sanchez C. 1988. Sol–gel chemistry of transition metal oxides. *Prog Solid State Chem* 18:259–342.
- Ma K. 1995. Microstructure of clay sediments or gels [Ph.D. thesis]. Edmonton, Canada: Univ of Alberta.
- Ma K, Pierre AC. 1992. Sedimentation behavior of a fine kaolinite in the presence of fresh Fe electrolyte: *Clays Clay Miner* 40:586–592.

- Michaels AS, Bolger JC. 1962. Settling rates and sediment volumes of flocculated kaolin suspensions. *IEC Fundam* 1: 24–33.
- Plitt LR. 1993. Mineral processing. Department of Mining, Metallurgical, and Petroleum Engineering. Edmonton, Canada: Univ of Alberta.
- Rand B, Melton IE. 1977. Particle interactions in aqueous kaolinite suspensions: I. Effect of pH and electrolyte upon the mode of particle interaction in homoionic sodium kaolinite suspensions. *J Colloid Interface Sci* 60:308–320.
- Rengasamy P, Oades JM. 1977. Interaction of monomeric and polymeric species of metal ions with clay surfaces. I: Adsorption of iron(III) species; II: Changes in surface properties of clays after addition of iron(III). *Aust J Soil Res* 15:221–242.
- Smart P, Tovey NY. 1982. Electron microscopy of soils and sediments: Techniques. Oxford: Clarendon Pr. 264 p.
- Schofield RK, Samson HR. 1954. Flocculation of kaolinite due to the attraction on oppositely charged crystal faces. *Discuss Faraday Soc* 18:135–145.
- Schwertmann U, Taylor RM. 1989. Iron oxides. In: Dixon JB, Weed SB, editors. Minerals in soil environments. Madison, WI: Soil Sci Soc Am. p 379–427.
- van Olphen H. 1977. An introduction to clay colloid chemistry. 2nd ed. New York: John Wiley. 318 p.
- Verwey EJW, Overbeek JTG. 1948. Theory of the stability of lyophobic colloids. New York: Elsevier. 205 p.
- Young RN, Ohtsubo M. 1987. Interparticle action and rheology of kaolinite–amorphous iron hydroxide (ferrihydrite) complexes. *Appl Clay Sci* 2:63–81.
- Zou J, Pierre AC. 1992. SEM observations of card-house structures in montmorillonite gels. *J Mater Sci Lett* 10:664–665.

(Received 16 August 1996; accepted 25 January 1997; Ms. 2805)